

Global Dynamics of the Advanced Light Source Revealed through Experimental Frequency Map Analysis

D. Robin and C. Steier

Lawrence Berkeley National Laboratory, 1 Cyclotron Road, Berkeley, California 94720

J. Laskar and L. Nadolski

Astronomie et Systèmes Dynamiques, IMC-CNRS, 77 avenue Denfert-Rochereau, 75014 Paris, France

(Received 27 December 1999)

Frequency map analysis was first used for the dynamical study of numerical simulations of physical systems (solar system, galaxies, particle accelerators). Here it is applied directly to the experimental results obtained at the Advanced Light Source. For the first time, the network of coupling resonances is clearly visible in an experiment, in a similar way as in the numerical simulation. Excellent agreement between numerical and experimental results leads us to propose this technique as a tool for improving numerical models and actual behavior of particle accelerators. Moreover, it provides a model-independent diagnostic for the evaluation of the dynamical properties of the beam.

PACS numbers: 29.27.Bd, 05.45.Ac, 05.45.Pq, 29.20.Lq

(I) Introduction.—The Advanced Light Source (ALS) is a third generation synchrotron light source located at Lawrence Berkeley National Laboratory [1]. High energy electrons produce synchrotron radiation as they circulate around its 200 m circumference storage ring. The magnets which are distributed around the ring form the magnetic lattice: dipoles for guiding the electrons, quadrupoles for focusing, and sextupoles for correction of chromatic aberrations of electron motion. Electrons with initial conditions that are not exactly on the central closed orbit will tend to oscillate about it, and the magnetic optics needs to be adjusted properly so that these oscillations remain stable. There are several reasons for this. First, one wants to be able to quickly fill the ring with electrons (“high injection efficiency”). One also wants the electrons to remain in the ring for many hours (“long beam lifetime”). Both injection efficiency and beam lifetime are affected by the stability of electron motion. If their motion at large amplitudes is unstable, electrons scattered to these large amplitudes via collisions with gas particles or other electrons may be lost. Similarly, electrons injected at large amplitude may not be captured. Thus high injection efficiency and long beam lifetimes require a large stable region in which electrons will survive.

As in other third-generation light sources, the ALS storage ring includes strongly focusing quadrupoles that are required to reduce the beam’s emittance. These quadrupole magnets generate large chromatic aberrations that must be corrected with sextupole magnets. The sextupoles in turn generate geometrical and nonlinear chromatic aberrations, exciting resonances that can make the motion of the electrons unstable. A resonance occurs when there is an integer relation between the horizontal and vertical betatron tunes ν_x, ν_y , and the longitudinal revolution frequency ν , which is normalized to $\nu = 1$, i.e.,

$$N_x \nu_x + N_y \nu_y + R = 0, \quad (1)$$

where N_x, N_y , and R are integers. If the lattice is M -fold periodic, its dynamics is the same as the dynamics of a single sector with longitudinal frequency $\nu' = M$. A resonance will occur only when $R = R' \times M$, that is, when R is evenly divisible by M . The ALS magnetic lattice is constructed of twelve identical sectors. This 12-fold periodicity will thus suppress many resonances.

(II) Frequency Map Analysis.—It is well known that resonances can lead to irregular and chaotic behavior for the orbits of particles, which eventually will get lost by diffusion in the outer parts of the beam, thus reducing its lifetime. It has therefore been a constant concern for accelerator dynamicists to design lattices in order to avoid resonances of low order ($|N_x| + |N_y|$) which are thought to be the most dangerous. Unfortunately, there is no simple way to forecast the real strength of a resonance without using a tracking code which numerically simulates the evolution of beam particles using a model of the lattice in which each element (quadrupole, sextupole, etc.) is represented by a different Hamiltonian of simple form [2]. The study of such noncontinuous Hamiltonian systems is performed using a surface of section corresponding to a fixed plane of given location in the lattice ($s = 0$, where s is the longitudinal position). The return map for this surface of section is a four-dimensional symplectic map with transverse positions (x, y) and momenta (p_x, p_y) as canonical coordinates.

The dynamics of this four-dimensional symplectic map is analyzed using Laskar’s frequency map analysis (FMA) method [3–7]. Briefly speaking, FMA constructs numerically a map from the space of initial conditions to the frequency space. More precisely, two of the initial conditions are fixed (here $x = y = 0$), and p_x, p_y are taken on a grid of initial conditions. For each selected initial condition (p_{x0}, p_{y0}) , the equations of motion of the particle are integrated numerically, and the evolution of the trajectory in the four-dimensional surface of section $s = 0$ is followed by recording the values of $x(t), y(t), p_x(t), p_y(t)$ over an

interval of time $[0, T]$. Then, using a numerical algorithm based on some refined Fourier technique (see [6]), we search for a quasiperiodic approximation of $z_x(t) = x(t) + ip_x(t)$ and $z_y(t) = y(t) + ip_y(t)$ of the form

$$z_w(t) = a_{w0}e^{i\nu_w t} + \sum_{k=1}^N a_{m_k}^w e^{i\langle m_k, \nu \rangle t}, \quad (2)$$

where $w = x, y$, $\nu = (\nu_x, \nu_y, 1)$, $m_k = (m_{1k}, m_{2k}, m_{3k})$ is a multi-index, and $\langle m_k, \nu \rangle = m_{1k}\nu_x + m_{2k}\nu_y + m_{3k}$. If the trajectory is a regular trajectory, KAM (Kolmogorov, Arnold, Moser) theory (see [8]) ensures that $z_w(t)$ is quasiperiodic of the form (2), with fundamental frequencies $(\nu_x, \nu_y, 1)$. In this case, the frequencies can be determined with very high accuracy since the algorithm converges asymptotically like $1/T^4$ to the true values [6]. Thus, on the set \mathcal{A} of initial momenta leading to regular KAM orbits, we can construct the frequency map $F : \mathcal{A} \subset \mathbf{R}^2 \rightarrow \mathbf{R}^2 : (p_{x0}, p_{y0}) \rightarrow (\nu_x, \nu_y)$ which associates the fundamental frequencies (ν_x, ν_y) to the initial momentum variables (p_{x0}, p_{y0}) of the corresponding orbit. Moreover, since the numerical algorithm always yields a quasiperiodic approximation of the trajectories, this map F is defined numerically on the entire space of initial momenta (p_{x0}, p_{y0}) . On the set of orbits which are not regular, the behavior of this map is unknown, but we are ensured that the frequency map is regular on the set \mathcal{A} of regular initial conditions, or more precisely, as this set is discontinuous, the restriction of the map to \mathcal{A} can be extended in a smooth diffeomorphism \tilde{F} on an open set B of \mathbf{R}^2 which coincides with F on \mathcal{A} [6,9]. We are thus ensured that when the map F is not regular, the orbits are chaotic, in the sense that they are not KAM quasiperiodic solutions. FMA also allows one to measure precisely the diffusion of orbits in the frequency space [4,5].

For practical use, FMA has the advantage of providing a clear and intuitive view of the global dynamics of the whole phase space of the system. This is illustrated by Fig. 1 which represents the image in the frequency plane (ν_x, ν_y) of a grid of initial momenta (p_{x0}, p_{y0}) with tracking over 1000 turns. This is about $1/20$ of the damping time due to synchrotron radiation which has been ignored in the computations. In the lattice model the chromaticity is adjusted to be slightly positive—which is how the real machine is operated. This is done using two families of sextupoles that exist in the storage ring. In Fig. 1, the lattice is supposed to be ideal, with a complete 12-fold periodicity. The working point, that is, the tunes at the center of the beam, is set to $(14.25, 8.18)$. As the initial amplitude of the particle increases, the tunes shift away from the working point. Initial conditions with zero vertical or horizontal amplitude correspond, respectively, to the lower-right and upper-left envelopes of the plot. The lines appearing in this figure are resonant lines revealed by the distortion of the frequency map. In the vicinity of these resonant lines appear chaotic zones corresponding to non-regular behavior of the frequency map.

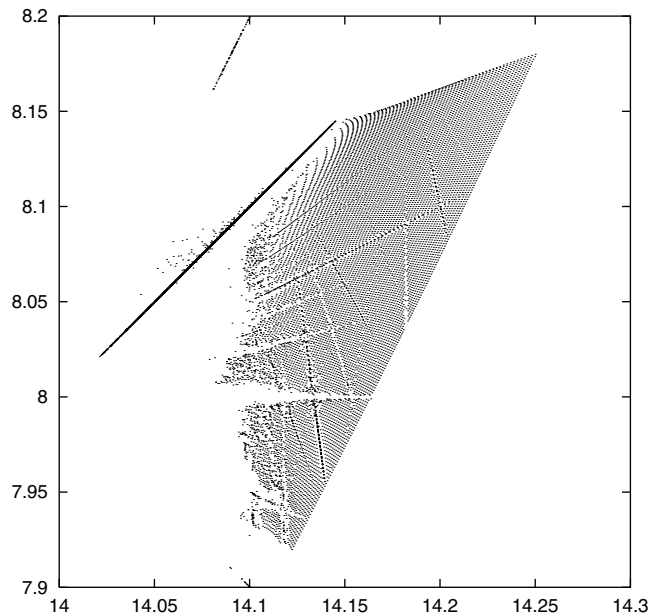


FIG. 1. Frequency map of the ALS for an ideal lattice.

For a number of reasons (e.g., errors in the manufacture of magnets) the machine is not perfect, and the existence of defects reduces the extent of the regular region by destroying the 12-fold periodicity and exciting resonances which appear only with very small amplitude in an ideal machine. Figure 2 shows the image of the frequency map for a realistic case, where the fitted linear (normal and coupling) magnetic errors have been included in the model [10]. It is clear that the stable region in this new model

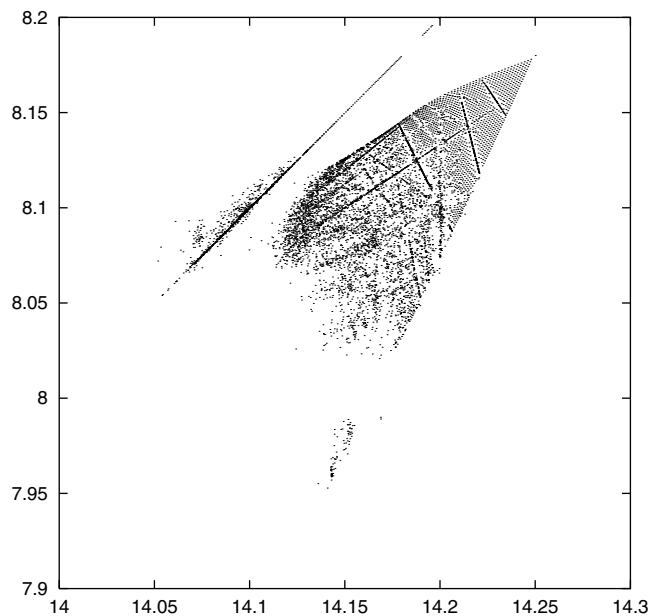


FIG. 2. Frequency map of the ALS for the lattice with measured errors.

is significantly reduced in comparison with the ideal lattice (Fig. 1). The reduction is most prominent for particles with large horizontal amplitude, as seen by a reduction in vertical extent of the map. It appears therefore that one of the main issues in particle accelerator dynamics is the search for a model which accurately describes the dynamics of real machines. This would allow one to compensate for the machine defects and to improve its performance. Ideally, one would like to observe the real dynamics of the beam while the machine is working. Indeed, at the ALS, it is now possible to obtain an experimental frequency map which provides for the first time a picture of the global dynamics of the real beam.

The ALS storage ring is equipped with two tools to perform measurements for the frequency map. The first tool is a set of two fast pulsing magnets called “pinger magnets.” Each pinger magnet’s pulse time is only 600 ns. This is less than the time it takes for electrons to execute one turn around the ring. Therefore these magnets can provide a “single-turn” transverse kick to the electrons. The first magnet (the horizontal pinger) provides only a vertical field, and similarly the second (the vertical pinger) provides only a horizontal field. The amplitudes of the horizontal and vertical fields may be adjusted independently. Together both pinger magnets are able to deliver a variable amplitude single-turn horizontal and vertical kick to the electron beam. The second tool used for frequency map measurement is a single-turn beam position monitor (BPM). Each turn, the BPM measures the transverse center of charge of the electron beam as it revolves around the ring. The BPM can store up to 1024 consecutive data and is synchronized with the pinger magnet pulse. In this way it is possible to record the beam position of the first 1024 turns after the beam is kicked by the pinger magnets.

(III) *Experimental conditions.*—During an experiment, the ring is filled with a train of electron bunches that extends over $1/8$ of the ring. The total current is 10 mA, which corresponds to 4×10^{10} electrons. The beam is kicked by the pinger magnets and the turn-by-turn position of the center of charge of the train of electron bunches is measured by the BPM.

During each experimental run, two sets of measurements are taken. The first data set is used to calibrate the linear model. The second one is a set of turn-by-turn data for the frequency map. During these measurements, in order to obtain a regularly distributed image, the square of the horizontal and vertical pinger strengths are evenly spaced. The data acquisition time for each point is about 20 sec, or about 4 hours for the 600 initial conditions of the frequency map.

For the first experiment the ALS storage ring was set up close to the nominal condition for operation. The betatron tunes were adjusted to $\nu_x = 14.25$ and $\nu_y = 8.18$, and the chromaticities to $\zeta_x = 0.5$, $\zeta_y = 1$. The linear magnetic lattice was measured and adjusted to make it as close to 12-fold periodic as possible. The frequency analysis was per-

formed with 25 by 25 initial conditions (Fig. 3a). The most striking feature of this plot is the very clear appearance of the two strongly excited coupling resonances of 5th order ($4\nu_x + \nu_y - 65 = 0$ and $3\nu_x + 2\nu_y - 59 = 0$). It is remarkable that these two resonances are “unallowed” resonances for the lattice. Indeed, they do not show up in the frequency map of the ideal machine (Fig. 1). These resonances are excited by small remaining coupling errors in the lattice that perturb the periodicity of the ring. In order to check the lattice model, we also performed FMA of the numerical simulation with a similar set of initial conditions (Fig. 3b). The agreement of the two results, experimental (Fig. 3a) and numerical (Fig. 3b), is excellent, which reflects the quality of the adjustment of the lattice model. In the future, we expect to reduce the acquisition time for the experimental frequency map, which could then be used as an interactive on-line monitor of the quality of the beam dynamics. It will immediately alert us to any unwanted features of the beam such as destroyed periodicity, or unusual working point.

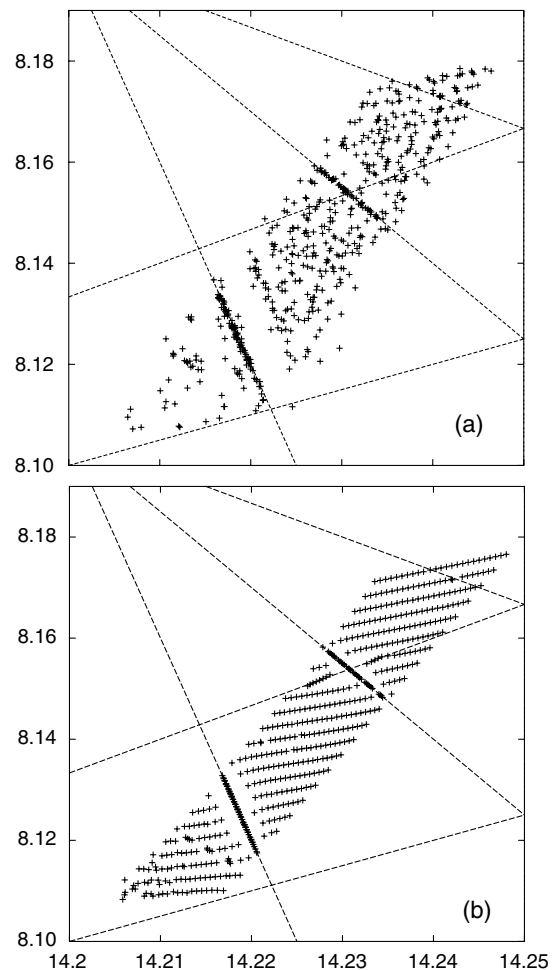


FIG. 3. Experimental frequency map (a), and numerical simulation (b) for the ALS with its current settings. Resonances of order ≤ 5 are plotted with dotted lines.

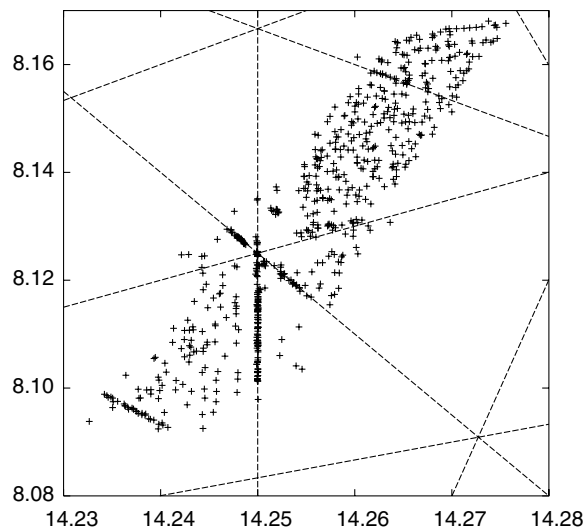


FIG. 4. Experimental frequency map for a previous setting of the ALS.

As an illustration, we set up the beam at a different working point ($\nu_x = 14.275$, $\nu_y = 8.167$). In this case, the experimental frequency map (Fig. 4) shows several unwanted resonances intersecting at ($\nu_x = 14.25$, $\nu_y = 8.125$). This intersection of active resonances will induce rapid diffusion of particles with subsequent decrease of the machine's performance. Indeed, we observed significant beam loss at this intersection during the experiment. It is clear that upon observing such behavior, one should either find a way to reduce the amplitude of resonances by improving the periodicity of the lattice or change the working point to another location. In fact, this working point was the designed ALS working point at which the machine was operated for several years. At this setting, the injection efficiency was somewhat erratic and the reason for this was not clearly understood at the time. The working point was changed to the present values after observation of the FMA of a previous numerical model of the lattice [7].

(IV) *Conclusions.*—Some experiments at other accelerators have used pinger/BPM systems to study nonlinear beam dynamics [11] and attempts have been made to relate FMA to measured frequencies [12,13]. But to our knowledge, we have presented here for the first time through an experiment the full network of coupling resonances occurring in such a Hamiltonian dynamical system of 3 degrees of freedom. This experiment clearly demonstrates how the complexity of the dynamics of such a system cannot be reduced to simple resonances of a 2 degrees of freedom system. This underscores the importance of understanding

the subtle behavior encountered in dynamical systems of 3 degrees of freedom (see [4] and references therein).

Yet it is remarkable that the numerical model (which is relatively simple) agrees so well with the observed dynamics. This gives us confidence that it may be used effectively to simulate modifications of the lattice, like insertion of new devices. We are convinced that the acquisition time for the experimental frequency map can be decreased significantly, and that this technique can be used in the future as a regular maintenance device for the ALS and similar machines.

This work was funded by the France-Berkeley Fund, CNRS, CEA, and by the D.O.E. under Contract No. DE-AC03-76SF00098. The authors thank the staff at the Advanced Light Source and particularly Alan Jackson and Ben Feinberg for their encouragement and support for this work, and Scott Dumas for suggesting improvements in the writing of the paper.

-
- [1] 1–2 GeV Synchrotron Radiation Source Conceptual Design Report, LBNL publication *PUB-5172 Rev.*, 1986.
 - [2] E. Forest, *Beam Dynamics* (Harwood Academic Publishers, Chur, Switzerland, 1998).
 - [3] J. Laskar, *Icarus* **88**, 266–291 (1990).
 - [4] J. Laskar, *Physica (Amsterdam)* **67D**, 257–281 (1993).
 - [5] H. S. Dumas and J. Laskar, *Phys. Rev. Lett.* **70**, 2975–2979 (1993).
 - [6] J. Laskar, in *Introduction to Frequency Map Analysis*, edited by C. Simó, NATO Advanced Study Institutes (Kluwer Academic Publishers, Dordrecht, The Netherlands, 1999).
 - [7] J. Laskar and D. Robin, *Part. Accel.* **54**, 183 (1996).
 - [8] V. Arnold, *Dynamical Systems III* (Springer-Verlag, Berlin, 1988).
 - [9] J. Pöschel, *Commun. Pure Appl. Math.* **25**, 653–695 (1982).
 - [10] D. Robin, J. Safranek, and W. Decking, *Phys. Rev. ST Accel. Beams* **2**, 044001 (1999).
 - [11] S. Y. Lee, in *Proceedings of the Nonlinear Beam Dynamics Workshop*, edited by M. Berz (IOP, Philadelphia, 1992), p. 249.
 - [12] A. Terebilo, C. Pellegrini, M. Cornacchia, J. Corbett, and D. Martin, in *Proceedings of the 1997 Particle Accelerator Conference, Vancouver, Canada* (IEEE, Piscataway, NJ, 1998), pp. 1457–1459.
 - [13] R. Bartolini, L. H. A. Leunissen, Y. Papaphilippou, F. Schmidt, and A. Verdier, in *Proceedings of the Particle Accelerator Conference, New York, 1999* (IEEE, Piscataway, NJ, 1999), pp. 1557–1559.